RNAi-mediated gene knockdown and anti-angiogenic therapy of RCCs using a cyclic RGD-modified liposomal-siRNA system.

Yu Sakurai[a], Hiroto Hatakeyama[a], Yusuke Sato[a], Mamoru Hyodo[a], Hidetaka Akita[a], Noritaka Ohga[b], Kyoko Hida[b], Hideyoshi Harashima[a]

[a] Laboratory of Innovative Nanomedicine, Faculty of Pharmaceutical Sciences, Hokkaido University, Kita 12, Nishi 6, Kita-ku, Sapporo 060–0812, Japan

[b] Division of Vascular Biology, Graduate School of Dental Medicine, Hokkaido University, Kita 13 Nishi 7, Kita-ku, Sapporo 060-0812, Japan

Correspondence should be addressed to Hideyoshi Harashima (harasima@pharm.hokudai.ac.jp)
Kita-12, Nishi-6, Kita-ku, Sapporo 060-0812, Japan. E-mail: harasima@pharm.hokudai.ac.jp
TEL: +81-11-706-3919
FAX: +81-11-706-4879

keyword: siRNA; liposome; anti-angiogenic therapy; cyclic RGD; active targeting

Abstract

Angiogenesis is one of crucial processes associated with tumor growth and development, and consequently a prime target for cancer therapy. Although tumor endothelial cells (TECs) play a key role in pathological angiogenesis, investigating phenotypical changes in neovessels when a gene expression in TEC is suppressed is a difficult task. Small interfering RNA (siRNA) represents a potential agent due to its ability to silence a gene of interest. We previously developed a system for *in vivo* siRNA delivery to cancer cells that involves a liposomal-delivery system, a MEND that contains a unique pH-sensitive cationic lipid, YSK05 (YSK-MEND). In the present study, we report on the development of a system that permits the delivery of siRNA to TECs by combining the YSK-MEND and a ligand that is specific to TECs. Cyclo(Arg-Gly-Asp-D-Phe-Lys) (cRGD) is a well-known ligand to $\alpha_v\beta_3$ integrin, which is selectively expressed at high levels in TECs. We incorporated cRGD into the YSK-MEND (RGD-MEND) to achieve an efficient gene silencing in TECs. Quantitative RT-PCR and the 5' rapid amplification of cDNA ends PCR indicated that the intravenous injection of RGD-MEND at a dose of 4.0 mg/kg induced a significant RNAi-mediated gene reduction in TEC but not in endothelial cells of other organs. Finally, we evaluated the therapeutic potency of the RGD-MEND encapsulating siRNA against vascular endothelial growth factor receptor 2. A substantial delay in tumor growth was observed after three sequential RGD-MEND injections on alternate days. In conclusion, the RGD-MEND represents a new approach for the characterization of TECs and for us in anti-angiogenic therapy.

Introduction

Angiogenesis is a major cause in cancer progression and metastasis[1, 2]. Folkman *et al.* first proposed the theory that, to be supplied with oxygen and other nutrients, tumors with sizes over 1-2 mm^3 inevitably required angiogenesis, and that, if tumor vasculature development could be inhibited, tumor tissue would shrink, as the result of a lack of oxygen and other nutrients[3]. Since this publication, anti-angiogenic therapy has evolved as an innovative treatment for various cancers. A mono-clonal antibody against vascular endothelial growth factor (VEGF), which is referred to as Avastin, is currently used in the treatment of various types of cancer[4, 5].

Small interfering RNA (siRNA) was predicted to be a potentially useful drug for this purpose, due to the ability to inhibit the expression of any genes of interest in a sequence-specific manner[6]. However, its instability in the blood and the low permeability of the plasma membrane requires drug delivery systems that target specific cells in order to achieve an effective therapy by siRNA[6, 7]. We previously developed a liposomal siRNA system, a multi functional nano-device (MEND)[8, 9]. In the past report, the use of a MEND composed of a pH-sensitive cationic lipid, YSK05 (YSK-MEND) caused a significant gene reduction in tumor tissue when intratumorally and intravenously injected into tumor-bearing mice[10, 11]. A number of pH sensitive siRNA carriers, such as liposomes [12, 13], polyplexes [14] and micelles [15], have been evaluated for use in tumor targeting. pH-sensitive carriers are generally thought to be more suitable for tumor targeting than conventional cationic carriers because of their highly specific fusiogenicity in acidic endosomes[16]. YSK05 consists of two linoleyl fatty acid chains and a tertiary amino group, which are responsible for pH-responsive fusiogenicity in endosomes. In this study, we incorporated a ligand that is specific to tumor endothelial cells (TECs) into YSK-MEND to achieve anti-angiogenic therapy using siRNA.

Cyclo (Arg-Gly-Asp-D-Phe-Lys) (cRGD) peptide is a well-validated ligand for $\alpha_V\beta_3$ integrin, which is highly and selectively expressed on the cell surface of TECs and some types of cancer cells themselves [17]. cRGD is a known antagonist of $\alpha_V\beta_3$ integrin, and the injection of free cRGD suppresses tumor progression in many cancers such as glioblastomas and lung cancer[18]. This is because $\alpha_V\beta_3$ integrin plays a key role in angiogenesis in tumor tissue[19]. Moreover, the cRGD peptide can be used for a variety of purposes, including cancer imaging and therapy by conjugating cRGD with imaging probes, anti-cancer agents or drug carriers[20]. Concerning the *in vivo* delivery of nu-

cleic acids using cRGD, several reports have appeared in which tumor growth was inhibited by the systemic injection of anti-tumor and/or anti-angiogenic oligonucleotides encapsulated in micells[21] and lipoplexes[22-24]. However, in almost all of those reports it was not clear whether siRNA was delivered to cancer cells and TECs, and no direct evidence showing that a gene reduction in TECs was mediated by RNA interference. In this study, we verified gene silencing by siRNA in TECs using quantitative RT-PCR (qRT-PCR) and rapid amplification of the 5' cDNA ends (5' RACE-PCR), which was the only method available for confirming RNAi-induced silencing[7].

We chose renal cell carcinomas (RCCs) as a therapeutic model cancer through inhibiting angiogenesis, since it is well known that RCCs effectively respond to anti-angiogenic therapy[25]. Since RCCs are known to respond poorly to conventional anti-cancer drugs, interleukin-2 and interferon-α injection are currently the standard treatment for patients with progressive RCCs[26]. In recent years, however, novel agents targeting angiogenesis pathways have been developed as the result in advances in our understanding of tumor biology. Actually, Afinitor and Toricel (mTOR inhibitors) and Sutent (a multi kinase inhibitor) are currently being applied for metastatic RCCs in addition to Avastin.

Although anti-angiogenic treatment has had significant therapeutic effects for cancer progress and metastasis, it has been reported that some patients are refractory or acquire resistance to VEGF inhibition[27]. Several mechanisms are thought to be involved in the resistance anti-angiogenic treatment by VEGF blockade. Compensation by other pro-angiogenic mechanisms, such as basic fibloblast growth factors (bFGF), platelet-derived growth factor (PDGF) and angiopoietins, appears to be a dominant factor in the development of acquired resistance to VEGF inhibition. Moreover, recent reports suggest that the recruitment of other cells, such as pericytes and bone marrow-derived myeloid cells, to tumor vessels is implicated in the resistance to anti-angiogenic therapy[28, 29]. A methodology that will permit the complete control any gene that is expressed in TECs is needed for further elucidating the mechanism of anti-angiogenic therapy resistance, and hence developing a better therapy that targets tumor angiogenesis. In the study, we report that the RGD-MEND represents an efficient siRNA delivery system for cancer treatment through anti-angiogenic therapy.

Materials and Methods

Materials

1,2-distearoyl-sn-glycerophosphocholine (DSPC), 1-palmitoyl-2-oleoyl-sn-glycerophosphoethanolamine (POPE), 1,2-dimyristoyl-sn-glycerol, methoxypolyethylene glycol$_{2,000}$ (PEG-DMG), 1,2-distearoyl-sn-glycerol, methoxypolyethylene glycol$_{2,000}$ (PEG-DSG) and N-hydroxysuccinimide -polyethylene glycol$_{2,000}$-1,2-disteaoyl-sn-glycerophosphoethanolamine (NHS-PEG-DSPE) were purchased NOF (Tokyo, Japan). Cholesterol (chol), RPMI-1640 medium and DMEM were obtained from SIGMA Aldrich (St. Louis, MO). Egg phosphatidyl choline (EPC) and 1,2-distearoyl-sn-grycelo, methoxy polyethylene glycol (PEG-DSPE) were purchased from Avanti Polar Lipids (Alabaster, AL). siRNAs were obtained from Hokkaido System Science Co., Ltd. (Sapporo, Japan). [^{3}H]-choresteryl hexadecyl ether (CHE) were purchased from PerkinElmer Life Science (Tokyo, Japan). DiI and DiD were purchased from Invitrogen (Carlsbad, CA)

Synthesis of cRGD conjugates

We synthesized cRGD-conjugated PEG (RGD-PEG) as previously reported[30]. In brief, cRGD peptide was incubated with NHS-PEG-DSPE in 20 mM phosphate buffered saline (pH 7.4, PBS) at 37°C for 12 h. The mixture was then subject to dialysis using Spectra Por 6 (MWCO 1,000 Da, Spectrum) to remove un-conjugated RGD. The molecular weight of the conjugate was determined by MALDI TOF-MS.

MEND preparation

YSK-MENDs were prepared as previously reported [10, 11]. Briefly, 1,500 nmol of YSK05, 750 nmol of POPE, 750 nmol chol and 150 nmol PEG-DMG were dissolved in 400 μL of 90% (v/v) aqueous tertiary butanol (t-BuOH). When the fluorescence was incorporated into the YSK-MENDs, 0.5 mol% (of the total lipid) DiD was added to the tubes and the organic solvent was removed by evaporation before the lipid solution was mixed. Two hundred μL of siRNA solution (concentration 0.8 mg/mL in 2 mM filter-sterilized citrate buffer (pH4.5)) was gradually added to the shaking lipid solution, and homogenous particles of liposomal siRNA were spontaneously formed by drastically diluting the siRNA-lipid mixture to 2 mL with 20 mM citrate buffer. The t-BuOH was

then removed by ultrafiltration. For RGD-modification, a RGD-PEG solution was incubated with a YSK-MEND solution at 60°C for 30 min at various molar ratios (RGD-PEG/total lipid of YSK-MEND). The YSK-MENDs were characterized by a Zetasizer Nano ZS ZEN3600 instrument (Malvern Instruments, Worchestershire, UK). The encapsulation efficiency and recovery ratio were calculated using RiboGreen (Invitrogen) as previously described[10]. siRNA encapsulation efficiency rate of all MENDs used in this study was over 90%. The sequences of the used siRNAs are shown in Supplemental Table S1

Cell culture

OS-RC-2 cells and HEK293T cells were cultured in RPMI-1640 and DMEM, respectively. These media were supplemented with 10% fetal bovine serum, penicillin (100 U/mL) and streptomycin (100 μg/mL). TECs, which were previously isolated by Ohga *et al.*[31], and HUVEC were cultured in EBM-2 medium supplemented with 2% FBS (v/v) and bullet kits (Lonza, Walkersville, MD). All cells were maintained at 37°C in a 5% CO_2 humidified atmosphere.

Evaluation of antigen expression

For evaluating the expression of $\alpha_V\beta_3$ integrin, 1.0×10^6 trypsinized cells were suspended in 1 mL of FACS buffer (0.5% bovine serum albumin and 0.1% sodium azide in 20 mM PBS), and the suspension centrifuged at 4°C for 4 min at 500 ×*g*. The cells were incubated in 100-fold diluted anti human $\alpha_V\beta_3$ integrin rat IgG (R&D systems, Minneapolis, MN) for 30 min on ice. The antibody solution was then removed by centrifugation and the cells were washed twice with 500 μL of FACS buffer. Two hundred-fold diluted Alexa633-labeled anti rat IgG goat F(ab') (Invitrogen) was added to the cells. The cells were washed twice with 500 μL of FACS buffer, and re-suspended in 1 mL of FACS buffer. The cell suspension was analyzed by FACSCalibur (Becton Dickinson, Franklin Lakes, NJ).

Animal Study

Male, 4-week-old ICR mice and BALB/cAJcl-*nu*/*nu* were purchased from Japan SLC (Shizuoka, Japan) and CLEA (Tokyo, Japan), respectively. For preparing OS-RC-2-bearing mice, 1.0×10^6 OS-RC-2 cells in 75 μL of sterilized PBS were inocu-

lated into anesthetized BALB/cAJcl-*nu*/*nu* mice on the right flank. The experimental protocols were reviewed and approved by the Hokkaido University Animal Care Committee in accordance with the Guide for the Care and Use of Laboratory Animals.

Confocal laser scanning microscopy (CLSM) to determine the localization in tumor tissue of the MEND

OS-RC-2-bearing mice were intravenously administered with 3.0 mg/kg of DiD labeled-YSK-MEND. FITC-labeled Isolectin B4 (Vector Laboratories, Burlingame, CA) were injected via the tail vein 10 min before collecting. Tumor tissue was excised 24 h after injection of the YSK-MENDs, and then fixed with 4% paraformaldehyde (PFA). Fixed tumor tissue was washed with 10%, 30% and 50% sucrose over night. Tumor tissue was embedded in OCT compound, and 16 μm thick slices were prepared on the slideglass SUPERFROST S9441 (MATUSNAMI) with CM-3050S (Leica, Wetzlar, Germany). Tumor slices were washed with PBS twice, and covered with a cover glass. The tumor slices were observed with a FV10i-LIV microscope.

Flowcytometry (FCM) analysis for the internalization of MEND into cells

To investigate the localization of the YSK-MENDs in tumor tissue after systemic injection, OS-RC-2 bearing mice were systemically injected with DiD labeled-YSK-MENDs at a dose of 3 mg/kg. Tumor tissue was collected 6 h after injection, and then shredded. The shredded tumor tissue was then incubated in 2 mL of Hanks' Balanced Salt Solution (HBSS, SIGMA Aldrich) containing 20 mg of type I collagenase (Gibco, Rockville, MD), 200 μg of DNase I (Gibco), 1 mL of inactivated FBS and 2.0 mmol of $CaCl_2$ for 30 min at 37°C. The resulting cell suspension was filtered through a 100 μm Cell Strainer (BD Falcon), and then centrifuged at 4°C for 3 min at 500 rpm after the addition of 10 mL of HBSS and the supernatant was removed. This "washing procedure" was repeated 2 times. To remove red blood cells, the centrifuged cells were incubated in Red Blood Cell Lysing Buffer (SIGMA Aldrich) for a several minutes at room temperature and the washing procedure was repeated once. Next, 1.0×10^6 cells were incubated with an anti mouse PE-labeled CD31 antibody (Biolegend, San Diego, CA) or PE-labeled Rat IgG2a, κ isotype control (Biolegend) for 30 min on ice. Cells were washed, and then analyzed with FACSCalibur 10 min after 7-AAD (IMGENEX, San Diego, CA) addition. The 7-AAD-positive population was assumed to be dead cells and were gated out.

Evaluation for gene silencing by qRT-PCR

Cells plated onto 6-well plate were lysed by treatment with 350 μL of TRIzol (Invitrogen). For the *in vivo* experiment, approximately 50 mg of collected tissue was homogenized by means of a PreCellys (Bertin Technologies, Montigny-Le-Bretonneux, France) in 500 μL of TRIzol, and then centrifuged at 12,000 ×*g* at 4°C for 15 min. Supernatant was used as an RNA extraction sample. RNA extraction and purification was then performed according to the manufacturers' protocol. One μg of total RNA was subjected to reverse transcription reaction using a High Capacity RNA-to-cDNA kit (Applied Biosystems, Foster City, CA).

Fifty-fold diluted cDNA was subject to qPCR with Fast SYBR Green Master Mix (Applied Biosystems) using LightCycler-480 (Roche Diagnostics, Germany). The reaction conditions were according to the manufacturer's protocol. The sequences of all primer sets in the experiment are shown in Supplemental Table S1.

Confirmation of RNAi-mediated gene silencing by 5' RACE-PCR

5' RACE-PCR for the detection of *Cd31* mRNA cleaved by si-*Cd31* was carried out as previously reported[11]. Briefly, GeneRacer Adaptor was ligated into cleaved *Cd31* mRNA, and then reverse transcribed with *Cd31* Gene Specific Primer by SuperScript III (Invitrogen). Next, cDNA was amplified by 2 times PCR (i.e. nested PCR) with 2 different sets of PCR primer (Ad5 outer and *Cd31* outer primers for the 1st PCR, and Ad5 inner and *Cd31* inner primers for the 2nd PCR). All oligonucleotides used in the procedure are shown in Supplemental Table S1.

Somatic and hepatic toxicity

Liver toxicity was evaluated 24 h after injection of the MEND at a dose of 3.0 mg/kg. Serum asparate aminotransferase (AST) and alanine aminotransferase (ALT) were measured using a transaminase CII test kit (Wako Pure Chemicals, Osaka, Japan) in accordance with manufacturer's instructions.

Statistical analysis

Comparisons between multiple treatments were made using one-way ANOVA, followed by the Bonferroni test. Pair-wise comparisons between treatments were made using a

Student's t-test. A p-value of <0.05 was considered significant.

Results

Preparation and characterization of YSK-MEND modified with RGD-PEG (RGD-MEND)

The expression of integrin $\alpha_V\beta_3$ in two cell lines was determined by FCM (Fig. 1).

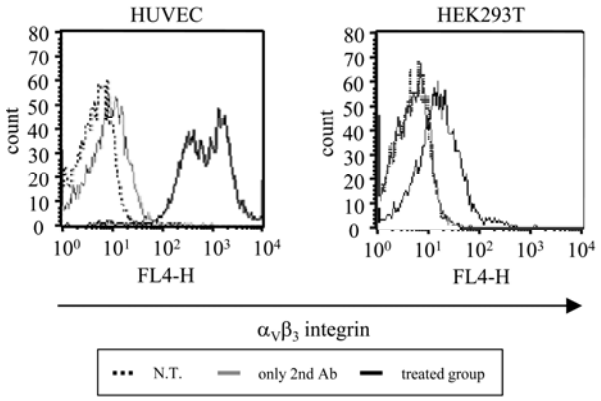

Fig. 1 $\alpha_V\beta_3$ integrin expression in HUVEC and HEK293T cells. HUVEC (left panel) and HEK293T (right panel) were treated with anti-$\alpha_V\beta_3$ integrin antibody and s fluorescence labeled-2nd antibody, and then analyzed by FCM. In the histograms, the black dotted line, the black solid line and the gray solid line denote untreated cells, cells treated with both the 1st and 2nd antibody and cells treated with only the 2nd antibody, respectively. N.T.: non treatment

We next evaluated the optimal modification ratio of RGD-PEG into the YSK-MEND at 0-10 mol% against the total lipid. The lipid composition of the YSK-MEND was YSK05/POPE/chol/PEG-DMG (50/25/25/3, molar ratio), which showed the most efficient silencing effect in the *in vitro* cultured cell line[10]. The PEG-DSPE (without cRGD) modified YSK-MEND (PEG-MEND) was regarded as a negative control in the *in vitro* study. The characteristics of these RGD-MENDs are shown in Table 1. In HUVEC, a 5.0 mol% modification facilitated the cellular internalization of the YSK-MEND to the greatest extent (Fig. 2). However, a further increase was not observed when the modification ratio was 10 mol% against the total lipid. On the other hand, no change in the cellular uptake of nanoparticles was observed in case of HEK293T cells. We also carried out this cellular uptake experiment with RGD-modified liposomes (Fig. S1), and similar results were observed in FCM and CLSM studies. Taken together, we conclude that the RGD-incorporation ratio was 5.0 mol%. In addition, RGD-modification had no effect on the pH-sensitivity of the YSK-MEND (Fig. S2). Next, we evaluated the knockdown effect

of RGD-MEND. Anti polo-like kinase 1 siRNA (si-*PLK1*) formulated into both RGD-MEND and PEG-MEND was added to HUVEC and HEK293T at a concentration of 11 – 100 nM. Anti-luciferase siRNA (si-*luc*) was used as a negative control siRNA. The RGD-MEND reduced target gene expression in a dose-dependent manner, while the PEG-MEND caused no detectable changes in target gene expression in HUVEC (Fig. 3A). In the case of HEK293T, however, neither the PEG-MEND nor the RGD-MEND induced gene silencing (Fig. 3B). On the other hand, si-*PLK1* transfection with RNAiMAX significantly inhibited *PLK1* expression in HEK293T cells (Fig. S3). This result clearly shows that HEK293T was not refractory to si-*PLK1*.

Table 1 Characteristics of the RGD-MENDs used in the *in vitro* cellular uptake experiments

	RGD-modified MEND				
lipid composition	YSK05/POPE/chol/PEG-DMG 50/25/25/3				
RGD-PEG (mol%)	0	1.0	2.5	5.0	10
diameter (nm)	106 ± 6	107 ± 8	106 ± 10	101 ± 3	110 ± 12
PdI	0.10 ± 0.02	0.15 ± 0.01	0.16 ± 0.04	0.13 ± 0.02	0.22 ± 0.05
ζ-potential (mV)	-5 ± 3	-6 ± 5	-9 ± 10	-11 ± 4	-13 ± 8

Data represents mean ± SD.

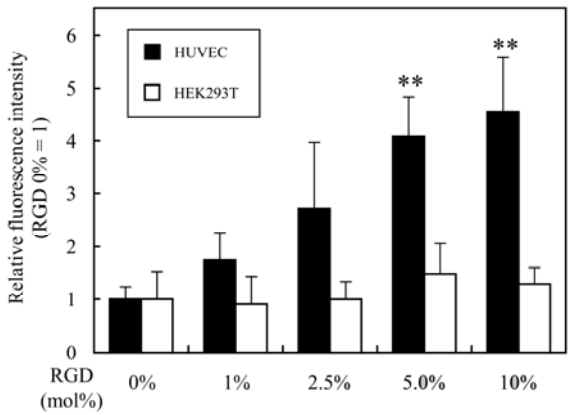

Fig. 2 Cellular uptake of RGD-MENDs containing various amounts of RGD-PEG. Cel-

lular uptake was determined by FCM at 3 h after adding the fluorescence-labeled MENDs to the cells. In the graph, the fluorescence intensity was normalized to RGD 0% in each cell line. White columns and black columns indicate the cellular uptake of HUVEC and that of HEK293T, respectively. **:p<0.01 (ANOVA followed by Bonferroni correction vs. RGD 0% in HUVEC. n=3).

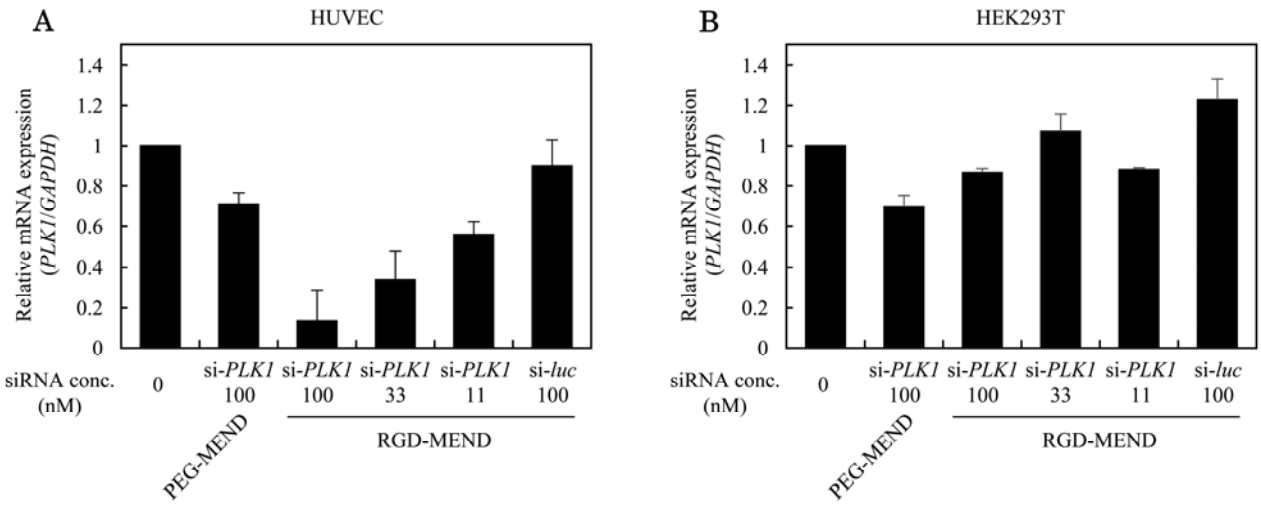

Fig. 3 Gene silencing effect of PEG-MEND and RGD-MEND. Cells were seeded on a 6-well plate 24 h prior to the MEND treatment, and the MENDs were then added to cells at the indicated concentrations for 24 h. Target gene mRNA expression was determined by qRT-PCR 24 h after the addition of PEG-MEND and RGD-MEND. *PLK1* expression was normalized to *GAPDH*.

Localization of RGD-MEND after systemically injection

We next investigated the tumor accumulation of RGD-MEND intravenously injected into mice. Tumor distribution was observed by CLSM and FCM in order to detect the specific delivery siRNA to TECs, not tumor whole tissue. To evaluate the targeting potency of the RGD-MEND, we compared with active targeting RGD-MEND with a "cancer cell targeting" YSK-MEND (a conventional YSK-MEND), which was originally developed for silencing cancer cell genes [11]. Generally speaking, liposomes with a prolonged circulation time after systemic injection can passively accumulate and diffuse in tumor tissue through the enhanced permeability and retention (EPR) effect[32]. The EPR effect is caused by increasing vessel permeability and decreasing lymphatic drainage in tumor tissue due to the development of an aberrant tumor vasculature. The

conventional YSK-MEND could circulate in blood stream as previously shown[11], and consequently accumulated and spread in tumor tissue. Therefore, the non-active targeting conventional YSK-MEND achieved "cancer cell targeting" via the EPR effect, which resulted in a significant gene silencing in cancer cells. In addition, we previously reported that non-ligand PEG-MEND (YSK05/POPE/chol/PEG-DMG 50/25/25/3) was not able to deliver siRNA in target organs, and concluded that the PEG-MEND could not be used as a negative control in the *in vivo* study. Taken together, in the *in vivo* section, the conventional YSK-MEND was regarded as a control non-TEC targeting carrier. The characteristics and lipid composition of the MENDs used in the *in vivo* experiments are shown in Table 2. Actually we were not able to observe the effective knockdown in TECs after the injection of the conventional YSK-MEND (Fig. S4). In TECs, the DiD signal was detected only in the group treated with the RGD-MEND (Fig. 4A). In addition, the RGD-MEMD was co-localized with TECs (Figs. 4B, S5). However, the intravenously injected conventional YSK-MEND was not observed in TECs but was diffused over the entire tumor tissue. To demonstrate the effect of cRGD, we also investigated the targeting ability and the knockdown efficiency of the PEG-MEND (YSK-MEND modified with PEG-DSPE instead of RGD-PEG). The systemically injected PEG-MEND neither accumulated in TECs (Fig. S6A) nor inhibited TECs-specific gene expression (Fig. S6B). Regarding the distribution in other organs, a high accumulation of systemically administered RGD-MEND was detected in the liver, spleen and lungs (Fig. S7).

Table 2 Characteristics of the YSK-MENDs used in the *in vivo* experiments

	RGD-MEND	PEG-MEND	conventional YSK-MEND
lipid composition	YSK05/POPE/chol/ PEG-DMG/RGD-PEG 50/25/25/3/5	YSK05/POPE/chol/ PEG-DMG/PEG-DSPE 50/25/25/3/5	YSK05/DSPC/chol PEG-DSG 50/10/40/3
diameter (nm)	115 ± 10	115 ± 17	105 ± 10
PdI	0.18 ± 0.01	0.21 ± 0.03	0.16 ± 0.04
ζ-potential (mV)	-18 ± 4	-18 ± 14	2.8 ± 1.4

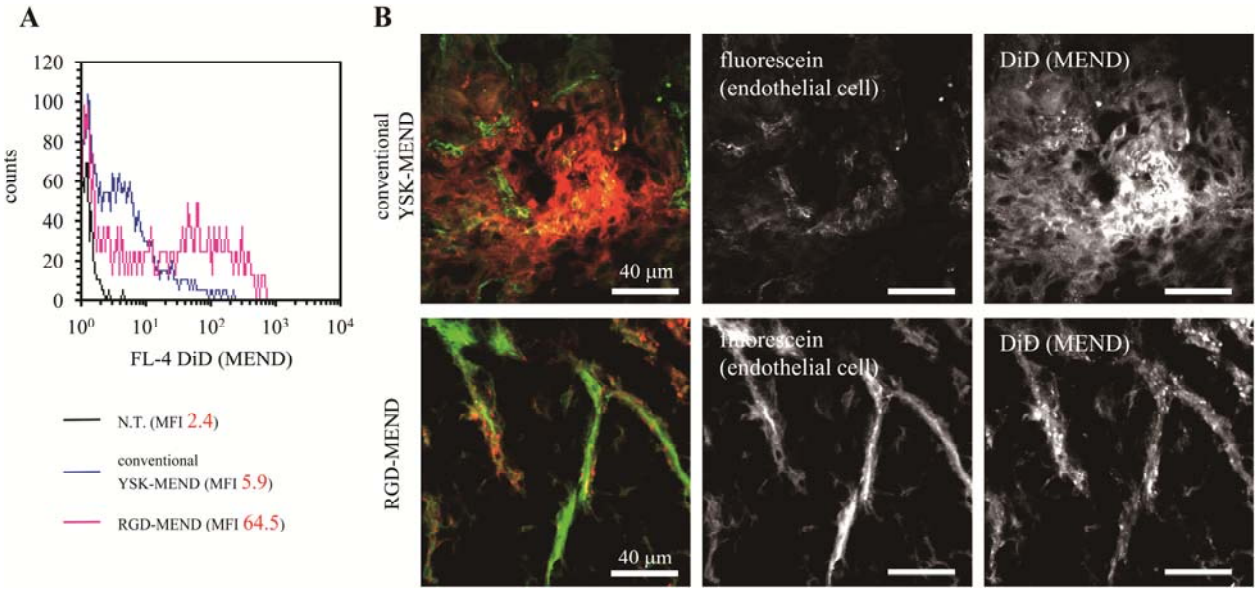

Fig. 4 Analysis of the localization of RGD-MEND in tumor tissue. Mean of the fluorescence intensity (MFI) of DiD in the CD31 positive population of tumor burden was compared among MENDs. B) DiD-labeled MENDs were injected into OS-RC-2-bearing mice, and 6 h after the injection, tumor tissues were collected and observed by CLSM. In merged images, green and red dots mean endothelial cells and MENDs, respectively. Upper panels show the images of conventional YSK-MEND and lower shows the images of RGD-MEND. Scale bars are 40 μm. N.T.: non treatment

Selective gene silencing of systemic administered RGD-MEND

We then evaluated the *in vivo* knockdown and therapeutic effect of the RGD-MEND. To specifically determine the extent of gene knockdown in TECs, *Cd31*, which is selectively expressed in both TECs and normal endothelial cells (ECs), was used. OS-RC-2-bearing mice were treated with anti *Cd31* siRNA (si-*Cd31*) encapsulated in the RGD-MEND at a dose ranging from 0.5 to 4.0 mg/kg. As a result, the RGD-MEND caused a reduction in *Cd31* expression in a dose-dependent manner while the si-*luc* encapsulated in RGD-MEND did not (Fig. 5A). In contrast, RGD-MEND did not downregulate the gene in cancer cells (Fig. S8). Furthermore, we confirmed that this inhibition was caused by RNAi with 5' RACE-PCR (Fig. 5B). As a result of a 5' RACE-PCR experiment, approximately 250 bp of PCR products were obtained at a dose of 4.0 mg/kg. Thus, the reduction in *Cd31* expression can be attributed to an RNAi-mediated mechanism (Fig. 5C). To evaluate the possibility that RGD-MEND injection causes side effects, we investigated the silencing effect of other organs' ECs. However, no inhibitory effect on the siR-

NA-target gene was observed in these tissues (Fig. S9)

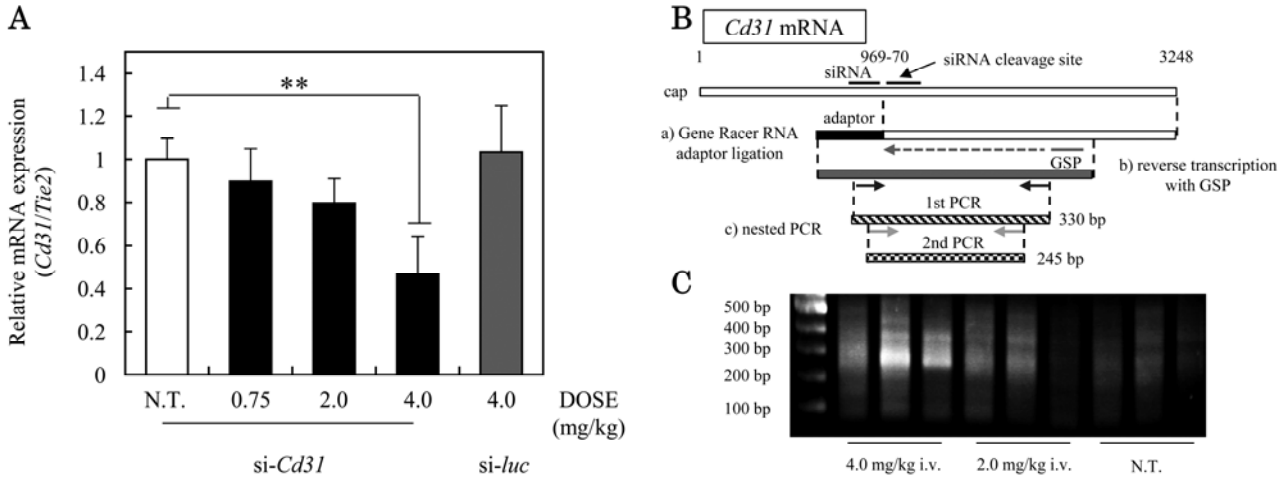

Fig. 5 Gene silencing via RNAi after injection of RGD-MEND. A) siRNA formulated in RGD-MEND was injected into OS-RC-2-bearing mice were injected at the indicated doses, and 24 h after the injection, *Cd31* expression was determined by qRT-PCR. B) Schematic diagram of the 5' RACE-PCR method. Predicted cleavage site by si-*Cd31* was *Cd31* mRNA (3,248 bp) and is indicated by an arrow between 969 and 970 bp of *Cd31 mRNA*. siRNA specific cleavage was detected as follows. First, the Gene Racer RNA adaptor was ligated into cleaved uncapped *Cd31* mRNA, and adaptor-ligated mRNA was then reverse transcribed with the gene specific primer (GSP). Next, complementary DNA was amplified by PCR with two independent primer sets (nested PCR). As a result, the production of 245 bp PCR fragment is indicative of siRNA-specific cleavage. C) The actual gel image of the 5' RACE-PCR products. RNA extracted from tumor-bearing mice which were treated with 4.0 or 2.0 mg/kg siRNA encapsulated in RGD-MEND was subjected to a 5' RACE-PCR procedure. N.T.: non treatment

Therapeutic effect of si-*Vegfr2* encapsulated in the RGD-MEND

Finally, we examined the therapeutic effect of the RGD-MEND. *VEGFR2* is one of the dominant factors in angiogenesis, and the inhibition of VEGFR2 by an antibody induced anti-tumor effect via thorough inhibition of angiogenesis including RCCs [33, 34]. Therefore, we chose *VEGFR2* as a therapeutic gene in this tumor model. The sequence of the anti *Vegfr2* siRNA was determined by comparing the gene silencing effect in cultured TECs (Fig. S10A). Then, OS-RC-2-bearing mice were daily injected twice with the most effective anti *Vegfr2* siRNA (si-*Vegfr2*) encapsulated in the RGD-MEND at a con-

centration of 3.0 mg/kg. As a result, a significant *Vegfr2* knockdown was observed *in vivo* (Fig. S10B). Additionally, si-*Vegfr2* had no effect on the viability of OS-RC-2 itself (Fig. S11). Then, when we monitored tumor growth after 3 injections of si-*Vegfr2* encapsulated in the RGD-MEND, a significant delay in tumor growth was observed (Fig. 6A). The si-*Vegfr2* treatment significantly lowered the amount of tumor wet tissue on day 17 compared to si-*luc* (Figs. 6B, C). To investigate whether *Vegfr2* suppression led to the inhibition of angiogenesis, vessels in tumor tissue were observed after 2 si-*Vegfr2* injections of 3.0 mg/kg by CLSM (Fig. 6D) The anti-angiogenesis effect was then evaluated by counting pixels indicating vessels, the vessels were significantly decreased in the si-*Vegfr2* group (Fig. 6E).

To evaluate the toxicity of systemically injected 3.0 mg/kg of RGD-MEND, we monitored changes in body weight during the treatment and also measured liver toxicity. No body weight change was observed in the OS-RC-2-bearing mice (Fig. 7A). Moreover, liposomal carriers sometimes severely injure the liver as liposomes tend to accumulate in liver. The activity of liver enzymes, AST and ALT, were not increased in the ICR mice at 24 h after the injection of 3.0 mg/kg MENDs (Fig. 7B).

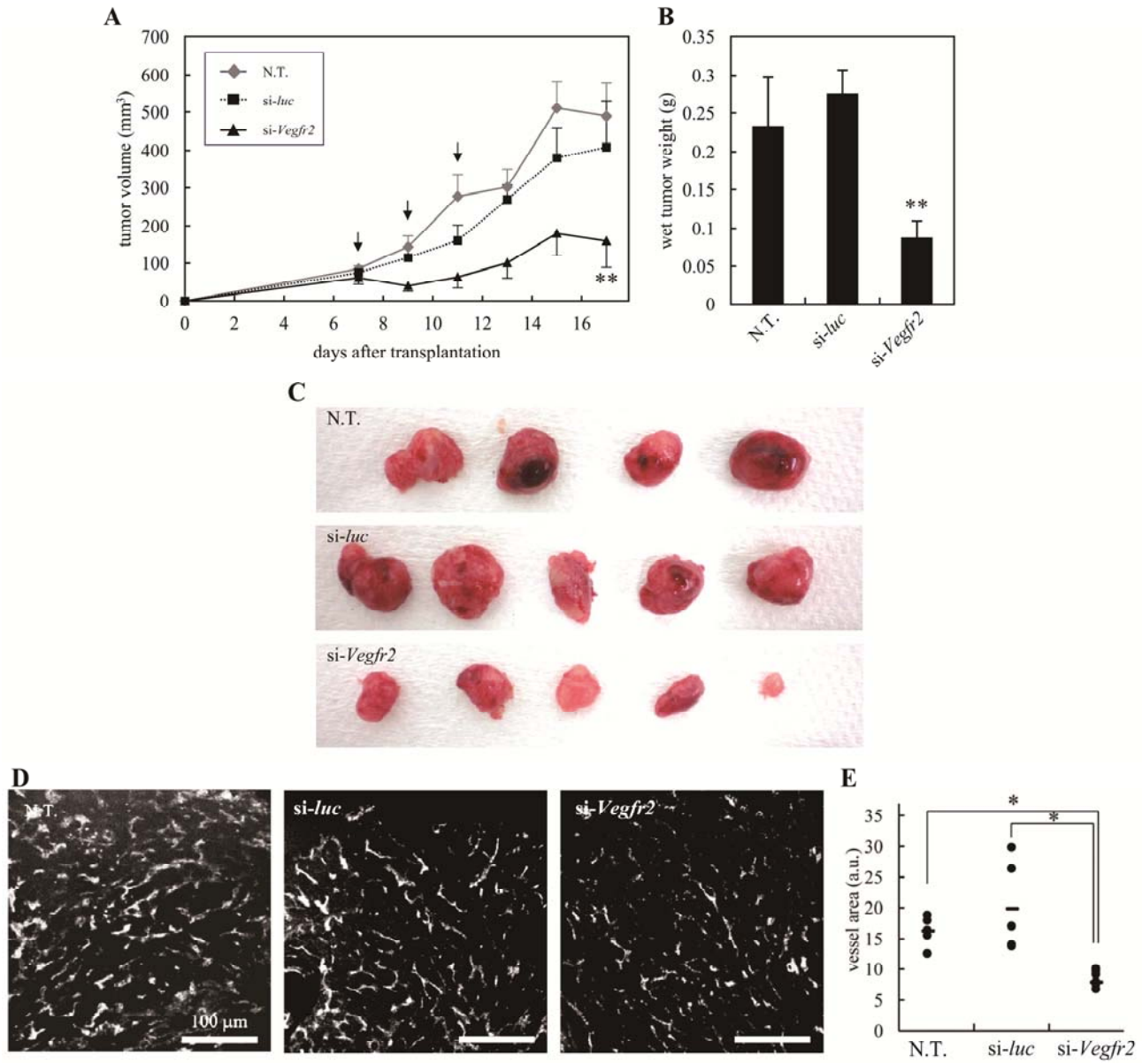

Fig. 6 Anti-tumor effect of si-*Vegfr2* encapsulated in RGD-MEND. A) RGD-MENDs encapsulating si-*luc* or si-*Vegfr2* were injected 3 times on alternate days at a dose of 3.0 mg/kg. Tumor volume was chronologically measured until day 17. Arrows denote the injection of the MEND. B) Wet tumor tissue was weighed when tumor was excised 17 days after transplantation. C) Photographs of collected tumor tissues. **: $p<0.05$ (ANOVA followed by Bonferroni correction vs. N.T., n=5) D) A typical image of each group is shown. Tumor bearing mice were injected with MENDs into tail vein twice. Twenty four h after the injection, tumor tissues were excised and observed with CLSM. Scale bars are 100 μm. E) Pixels showing vessels, which were stained by isolectin B4, were counted with ImageJ. *; $p<0.05$: ANOVA followed by SNK test, n=5-7. N.T.: non treatment

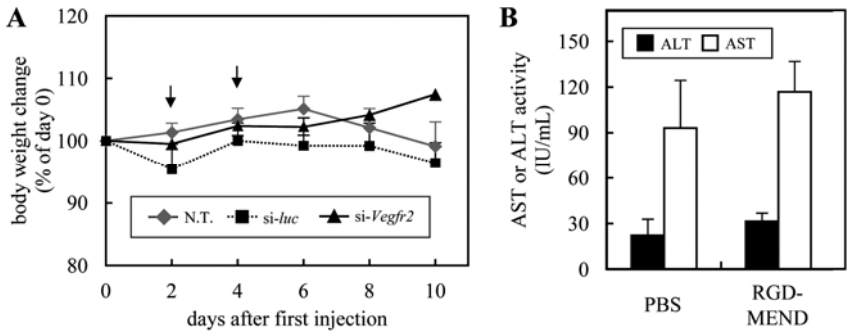

Fig. 7 Somatic and liver toxicological analysis of the RGD-MEND. A) The change in body weight was monitored after the first therapeutic injections into nude mice at a dose of 3.0 mg/kg every other day. Arrows show MENDs injection. B) Liver toxicity was evaluated by measuring the activities of selected liver enzymes, namely, ALT (black column) and AST (white column). These assays were performed 24 h after the injection of the RGD-MEND at a dose of 3.0 mg/kg. n=3. N.T.: non treatment

Discussion

The cRGD peptide is a well-known ligand for both cancer cells and TECs. Although cRGD has been widely used as a targeting ligand for oligonucleotide delivery to TECs, there are few reports directly showing TECs-specific gene silencing mediated by siRNA. In this study, we verified that the RGD-MEND is capable of inducing siRNA-mediated gene silencing in TECs and attempted to develop a cancer therapy through an anti-angiogenic effect by delivering siRNA.

As previously described, the apparent pKa of the carrier is a dominant factor for escaping from endosomes in pH responsive carriers [10]. After internalization via endocytosis, the YSK-MEND is rapidly converted into a cationic molecule in response to acidification in the endosomes, and, consequently, the endosomal membrane is disrupted by interacting with endosomal membranes with a negative charge. Therefore, it is important to adjust the pKa of the particle to around 6.5 in order to rapidly respond the declining pH in endosomes. The apparent pKa of the RGD-MEND was compared with the RGD-modified MEND. As a result, the pKa was around 6.5 and remained unchanged as the result of the modification of RGD (Fig S2). This suggests that the RGD-MEND would be able to efficiently escape from the endosome in response to endosome acidification after internalization mediated by $\alpha_V\beta_3$ integrin – RGD interaction. Five mol% of RGD-modification resulted in the maximum cellular uptake in HUVEC cells, whereas additional RGD-modification had no further effect on uptake. This saturation might be due to fixed quantity of $\alpha_V\beta_3$ integrin present on HUVEC cells. In addition, it was previously reported that the PEGylation ratio in liposomes was, at most, 5.0 mol%[35]. Collectively, 5.0 mol% of RGD-PEG might be the optimized modification condition in both aspects of cells and siRNA carriers.

The above mentioned properties on internalization via $\alpha_V\beta_3$ integrin and pH responsive fusiogenicity allows RGD-MEND to achieve a significant level of gene silencing in TECs at a dose of si-*Cd31* 4.0 mg/kg (Fig. 5). Nevertheless, gene silencing was saturated at 50% of N.T. In addition, two injections of 4.0 mg/kg of the RGD-MEND failed to drastically improve gene silencing (data not shown). This saturation might be caused by a limited distribution of the RGD-MEND in tumor tissue. When the distribution in tumor tissue was measured after systemic injection of the RGD-MEND, the fluorescence derived from the RGD-MEND was detected in approximately 80% of the TECs (Fig. S5). As the tumor vasculature is more heterogenous than normal tissue, blood flow is not

sufficient in some parts of tumor vessels [36, 37]. This heterogeneity in blood flow could lead to a limited distribution of the systemically delivered RGD-MEND.

As gene silencing in endothelial cells in normal organs would cause undesirable adverse effects, we determined the extent of accumulation in plasma, liver, spleen, kidney and lung by the RI-labeled not-PEGylated YSK-MEND (MEND), the PEG-MEND and the RGD-MEND containing RIs were injected into ICR mice, and the radio activity of these tissues were then measured (Fig. S7). Only the PEG-MEND showed a prolonged circulation time, while the others did not. Notably, a significant increased accumulation of RGD-MEND was observed in the spleen and lungs. The MEND accumulated most highly in the liver of three MENDs. The increased accumulation in the spleen can be attributed to platelets, which are abundant in the spleen. Platelets express $\alpha_{II\beta}\beta_3$ integrin, which has a relatively similar structure to $\alpha_V\beta_3$ integrin [38]. As cRGD can also weakly bind to the $\alpha_{II\beta}\beta_3$ integrin, the RGD-MEND may have accumulated in spleen. Though the mechanism responsible for the high accumulation of RGD-MEND in lungs is currently unclear, the cRGD conjugated oligopeptide-plasmid DNA complex also accumulated at slightly higher levels in the lung compared to the un-modified version used in a previous report[39]. Thus, a modest higher accumulation in the lung must be accompanied by cRGD modification. Taking into consideration the fact that the highest accumulation was in the liver and an increased accumulation was found in the lungs and spleen, *Cd31* gene silencing in these organs were evaluated 24 h after injection of the RGD-MEND. No significant gene reduction was observed in any of these organs (Fig. S9). Although a modestly higher accumulation of the RGD-MEND in the spleen and lungs was observed, there is little possibility that the systemic injection of RGD-MEND induced side effects in other organs. In the case of present anti-angiogenic agents, the inhibitory effect on angiogenesis in normal tissue, except for tumor tissue, can lead to an unfavorable influence. For example, Avastin can induce mortal side effects, such as bowel perforation and pulmonary hemorrhages because Avastin can inhibit VEGF signaling in normal tissue, which is required for the maintenance of healthy blood vessels[40, 41]. In contrast, since the RGD-MEND could selectively suppress gene expression in tumor tissue, its use should be safer than the currently used anti-angiogenic agents.

Although OS-RC-2 cells were $\alpha_V\beta_3$ integrin positive (data not shown), no significant knockdown was observed in cancer cells (Fig. S8). The failure of cancer cell gene si-

lencing was probably due to the lack of spreading of RGD-MEND in tumor tissue. Actually, almost all of the RGD-MEND appeared to remain in tumor vessels in the CLSM result (Fig. 5B). Although long-circulating liposomes can accumulate in tumor tissue after intravenous administration via the EPR effect as described above, the RGD-MEND failed to accumulate and diffuse in tumor tissue because of the instability of the RGD-MEND in the bloodstream (Fig. S7).

Although some groups reported on the therapeutic effect of cRGD itself, the injection of RGD-MEND encapsulating si-*luc* failed to inhibit tumor growth (Fig. 6A). In the reports dealing with the therapeutic effects of cRGD, the dosage of cRGD was 10-30 mg/kg [19, 42, 43]. On the other hand, the amount of cRGD was 1.6 mg/kg in the case of 4.0 mg/kg of cRGD-MEND. These facts suggest that the amount of cRGD on the RGD-MEND was insufficient to produce a curative effect. In contrast, tumor growth in the group treated with si-*Vegfr2* was markedly delayed. To exclude the possibility that si-*Vegfr2* led to cell death in OS-RC-2 cells themselves, we examined the effect of si-*Vegfr2* transfection to OS-RC-2 cells on viability. When OS-RC-2 cells were treated with si-*Vegfr2* and si-*luc*, no detectable reduction in cell viability compared to N.T. was found in both groups (Fig. S11). These results suggest that the injection of si-*Vegfr2* inhibits tumor growth via angiogenic gene knockdown in TECs.

Conclusions

The RGD-MEND caused significant gene silencing in tumor endothelial cells, but not in endothelial cells in normal organs and cancer cells without severe toxicity. In addition, 5' RACE-PCR revealed that siRNA-mediated RNA interference was responsible for the gene reduction observed in TECs. In other words, we succeeded in developing an efficient system for the delivery of siRNA specifically to tumor endothelial cells. This system is a promising siRNA delivery system for investigations of the pathological characteristics of tumor endothelial cells, and moreover for cancer treatment via controlling the biological function of tumor endothelial cells.

Acknowledgements

The authors also wish to thank Dr. Milton S. Feather for his helpful advice in writing the English manuscript.

Grant Support

This study was supported in part by a Grant-in-Aid for Scientific Research on Innovative Areas “Nanomedicine Molecular Science” (No. 2306) from Ministry of Education, Culture, Sports, Science, and Technology (MEXT) of Japan, and the Special Education and Research Expenses of the Ministry of Education, Culture, Sports, Science and Technology (MEXT) of Japan.

References

[1] N. Ferrara,R.S. Kerbel, Angiogenesis as a therapeutic target, Nature. 438 (2005) 967-974.

[2] L.M. Ellis,D.J. Hicklin, VEGF-targeted therapy: mechanisms of anti-tumour activity, Nat Rev Cancer. 8 (2008) 579-591.

[3] J. Folkman, Tumor angiogenesis: therapeutic implications, N Engl J Med. 285 (1971) 1182-1186.

[4] C. Harrison, Angiogenesis: A deeper understanding of VEGFR inhibitors, Nat Rev Cancer. 12 (2012) 735.

[5] C. Harrison, Anticancer drugs: A deeper understanding of VEGFR inhibitors, Nat Rev Drug Discov. 11 (2012) 831.

[6] K.A. Whitehead, R. Langer, D.G. Anderson, Knocking down barriers: advances in siRNA delivery, Nat Rev Drug Discov. 8 (2009) 129-138.

[7] G.R. Rettig,M.A. Behlke, Progress toward in vivo use of siRNAs-II, Mol Ther. 20 (2012) 483-512.

[8] K. Kogure, H. Akita, Y. Yamada, H. Harashima, Multifunctional envelope-type nano device (MEND) as a non-viral gene delivery system, Adv Drug Deliv Rev. 60 (2008) 559-571.

[9] H. Hatakeyama, H. Akita, H. Harashima, A multifunctional envelope type nano device (MEND) for gene delivery to tumours based on the EPR effect: a strategy for overcoming the PEG dilemma, Adv Drug Deliv Rev. 63 (2011) 152-160.

[10] Y. Sato, H. Hatakeyama, Y. Sakurai, M. Hyodo, H. Akita, H. Harashima, A pH-sensitive cationic lipid facilitates the delivery of liposomal siRNA and gene silencing activity in vitro and in vivo, J Control Release. 163 (2012) 267-276.

[11] Y. Sakurai, H. Hatakeyama, Y. Sato, M. Hyodo, H. Akita, H. Harashima, Gene Silencing via RNAi and siRNA Quantification in Tumor Tissue Using MEND, a Liposomal siRNA Delivery System, Mol Ther (2013).

[12] A.D. Judge, M. Robbins, I. Tavakoli, J. Levi, L. Hu, A. Fronda, E. Ambegia, K. McClintock, I. MacLachlan, Confirming the RNAi-mediated mechanism of action of siRNA-based cancer therapeutics in mice, J Clin Invest. 119 (2009) 661-673.

[13] S.C. Semple, A. Akinc, J. Chen, A.P. Sandhu, B.L. Mui, C.K. Cho, D.W. Sah, D. Stebbing, E.J. Crosley, E. Yaworski, I.M. Hafez, J.R. Dorkin, J. Qin, K. Lam, K.G. Rajeev, K.F. Wong, L.B. Jeffs, L. Nechev, M.L. Eisenhardt, M. Jayaraman, M. Kazem, M.A. Maier, M. Srinivasulu, M.J. Weinstein, Q. Chen, R. Alvarez, S.A. Barros, S. De, S.K. Klimuk, T. Borland, V. Kosovrasti, W.L. Cantley, Y.K. Tam, M. Manoharan, M.A. Ciufolini, M.A. Tracy, A. de Fougerolles, I. MacLachlan, P.R. Cullis, T.D. Madden, M.J. Hope, Rational design of cationic lipids for siRNA delivery, Nat Biotechnol. 28 (2010) 172-176.

[14] M. Meyer, A. Philipp, R. Oskuee, C. Schmidt, E. Wagner, Breathing life into polycations: functionalization with pH-responsive endosomolytic peptides and polyethylene glycol enables siRNA delivery, J Am Chem Soc. 130 (2008) 3272-3273.
[15] H. Yu, Y. Zou, Y. Wang, X. Huang, G. Huang, B.D. Sumer, D.A. Boothman, J. Gao, Overcoming endosomal barrier by amphotericin B-loaded dual pH-responsive PDMA-b-PDPA micelleplexes for siRNA delivery, ACS Nano. 5 (2011) 9246-9255.
[16] V.P. Torchilin, Recent advances with liposomes as pharmaceutical carriers, Nat Rev Drug Discov. 4 (2005) 145-160.
[17] C.J. Avraamides, B. Garmy-Susini, J.A. Varner, Integrins in angiogenesis and lymphangiogenesis, Nat Rev Cancer. 8 (2008) 604-617.
[18] C. Mas-Moruno, F. Rechenmacher, H. Kessler, Cilengitide: the first anti-angiogenic small molecule drug candidate design, synthesis and clinical evaluation, Anticancer Agents Med Chem. 10 (2010) 753-768.
[19] P.C. Brooks, A.M. Montgomery, M. Rosenfeld, R.A. Reisfeld, T. Hu, G. Klier, D.A. Cheresh, Integrin alpha v beta 3 antagonists promote tumor regression by inducing apoptosis of angiogenic blood vessels, Cell. 79 (1994) 1157-1164.
[20] F. Danhier, A. Le Breton, V. Preat, RGD-based strategies to target alpha(v) beta(3) integrin in cancer therapy and diagnosis, Mol Pharm. 9 (2012) 2961-2973.
[21] R.J. Christie, Y. Matsumoto, K. Miyata, T. Nomoto, S. Fukushima, K. Osada, J. Halnaut, F. Pittella, H.J. Kim, N. Nishiyama, K. Kataoka, Targeted polymeric micelles for siRNA treatment of experimental cancer by intravenous injection, ACS Nano. 6 (2012) 5174-5189.
[22] E. Kenjo, T. Asai, N. Yonenaga, H. Ando, T. Ishii, K. Hatanaka, K. Shimizu, Y. Urita, T. Dewa, M. Nango, H. Tsukada, N. Oku, Systemic delivery of small interfering RNA by use of targeted polycation liposomes for cancer therapy, Biol Pharm Bull. 36 (2013) 287-291.
[23] T. Tagami, T. Suzuki, M. Matsunaga, K. Nakamura, N. Moriyoshi, T. Ishida, H. Kiwada, Anti-angiogenic therapy via cationic liposome-mediated systemic siRNA delivery, Int J Pharm. 422 (2012) 280-289.
[24] S. Anand, B.K. Majeti, L.M. Acevedo, E.A. Murphy, R. Mukthavaram, L. Scheppke, M. Huang, D.J. Shields, J.N. Lindquist, P.E. Lapinski, P.D. King, S.M. Weis, D.A. Cheresh, MicroRNA-132-mediated loss of p120RasGAP activates the endothelium to facilitate pathological angiogenesis, Nat Med. 16 (2010) 909-914.
[25] D.Y. Heng,R.M. Bukowski, Anti-angiogenic targets in the treatment of advanced renal cell carcinoma, Curr Cancer Drug Targets. 8 (2008) 676-682.
[26] B. Escudier, Emerging immunotherapies for renal cell carcinoma, Ann Oncol. 23 Suppl 8 (2012) viii35-40.
[27] G. Bergers,D. Hanahan, Modes of resistance to anti-angiogenic therapy, Nat Rev

Cancer. 8 (2008) 592-603.
[28] J.S. Ko, P. Rayman, J. Ireland, S. Swaidani, G. Li, K.D. Bunting, B. Rini, J.H. Finke, P.A. Cohen, Direct and differential suppression of myeloid-derived suppressor cell subsets by sunitinib is compartmentally constrained, Cancer Res. 70 (2010) 3526-3536.
[29] I. Helfrich, I. Scheffrahn, S. Bartling, J. Weis, V. von Felbert, M. Middleton, M. Kato, S. Ergun, D. Schadendorf, Resistance to antiangiogenic therapy is directed by vascular phenotype, vessel stabilization, and maturation in malignant melanoma, J Exp Med. 207 (2010) 491-503.
[30] G. Kibria, H. Hatakeyama, N. Ohga, K. Hida, H. Harashima, Dual-ligand modification of PEGylated liposomes shows better cell selectivity and efficient gene delivery, J Control Release. 153 (2011) 141-148.
[31] N. Ohga, K. Hida, Y. Hida, C. Muraki, K. Tsuchiya, K. Matsuda, Y. Ohiro, Y. Totsuka, M. Shindoh, Inhibitory effects of epigallocatechin-3 gallate, a polyphenol in green tea, on tumor-associated endothelial cells and endothelial progenitor cells, Cancer Sci. 100 (2009) 1963-1970.
[32] H. Maeda, Y. Matsumura, H. Kato, Purification and identification of [hydroxyprolyl3]bradykinin in ascitic fluid from a patient with gastric cancer, J Biol Chem. 263 (1988) 16051-16054.
[33] R.A. Brekken, J.P. Overholser, V.A. Stastny, J. Waltenberger, J.D. Minna, P.E. Thorpe, Selective inhibition of vascular endothelial growth factor (VEGF) receptor 2 (KDR/Flk-1) activity by a monoclonal anti-VEGF antibody blocks tumor growth in mice, Cancer Res. 60 (2000) 5117-5124.
[34] I.J. Duignan, E. Corcoran, A. Pennello, M.J. Plym, M. Amatulli, N. Claros, M. Iacolina, H. Youssoufian, L. Witte, S. Samakoglu, J. Schwartz, D. Surguladze, J.R. Tonra, Pleiotropic stromal effects of vascular endothelial growth factor receptor 2 antibody therapy in renal cell carcinoma models, Neoplasia. 13 (2011) 49-59.
[35] K. Sou, T. Endo, S. Takeoka, E. Tsuchida, Poly(ethylene glycol)-modification of the phospholipid vesicles by using the spontaneous incorporation of poly(ethylene glycol)-lipid into the vesicles, Bioconjug Chem. 11 (2000) 372-379.
[36] P. Vaupel, F. Kallinowski, P. Okunieff, Blood flow, oxygen and nutrient supply, and metabolic microenvironment of human tumors: a review, Cancer Res. 49 (1989) 6449-6465.
[37] A.R. Pries, A.J. Cornelissen, A.A. Sloot, M. Hinkeldey, M.R. Dreher, M. Hopfner, M.W. Dewhirst, T.W. Secomb, Structural adaptation and heterogeneity of normal and tumor microvascular networks, PLoS Comput Biol. 5 (2009) e1000394.
[38] F. Bianchini, N. Cini, A. Trabocchi, A. Bottoncetti, S. Raspanti, E. Vanzi, G. Menchi, A. Guarna, A. Pupi, L. Calorini, (1)(2)(5)I-radiolabeled morpholine-containing arginine-glycine-aspartate (RGD) ligand of alphavbeta(3) integrin as a molecular

imaging probe for angiogenesis, J Med Chem. 55 (2012) 5024-5033.
[39] Y. Aoki, S. Hosaka, S. Kawa, K. Kiyosawa, Potential tumor-targeting peptide vector of histidylated oligolysine conjugated to a tumor-homing RGD motif, Cancer Gene Ther. 8 (2001) 783-787.
[40] T. Eisen, C.N. Sternberg, C. Robert, P. Mulders, L. Pyle, S. Zbinden, H. Izzedine, B. Escudier, Targeted therapies for renal cell carcinoma: review of adverse event management strategies, J Natl Cancer Inst. 104 (2012) 93-113.
[41] S. Goel, D.G. Duda, L. Xu, L.L. Munn, Y. Boucher, D. Fukumura, R.K. Jain, Normalization of the vasculature for treatment of cancer and other diseases, Physiol Rev. 91 (2011) 1071-1121.
[42] F. Mitjans, T. Meyer, C. Fittschen, S. Goodman, A. Jonczyk, J.F. Marshall, G. Reyes, J. Piulats, In vivo therapy of malignant melanoma by means of antagonists of alphav integrins, Int J Cancer. 87 (2000) 716-723.
[43] M.A. Buerkle, S.A. Pahernik, A. Sutter, A. Jonczyk, K. Messmer, M. Dellian, Inhibition of the alpha-nu integrins with a cyclic RGD peptide impairs angiogenesis, growth and metastasis of solid tumours in vivo, Br J Cancer. 86 (2002) 788-795.